Research Square

Preprints are preliminary reports that have not undergone peer review.
They should not be considered conclusive, used to inform clinical practice,
or referenced by the media as validated information.

Calcium Signaling Enhances Bostrycin Biosynthesis in Nigrospora sphaerica HCH285: Transcriptomic Insights into Metabolic Regulation

Boya Yang
Wuhan Polytechnic University
Sishang Zhang
Wuhan Polytechnic University
Zhangqian Wang
wzqsnu@whpu.edu.cn
Wuhan Polytechnic University
Feng Xu
Yangtze University
Wenyi Zhong
Wuhan Polytechnic University
Yizhou Liu
Wuhan Polytechnic University
Xingxing Dong
Wuhan Polytechnic University
Yi He
Wuhan Polytechnic University

Research Article

Keywords:

Posted Date: November 13th, 2026

DOI: https://doi.org/10.21203/rs.3.rs-11147586/v1

License: This work is licensed under a Creative Commons Attribution 4.0 International License.
Read Full License

Additional Declarations: No competing interests reported.

Calcium Signaling Enhances Bostrycin Biosynthesis in *Nigrospora sphaerica* HCH285: Transcriptomic Insights into Metabolic Regulation

Boya Yang[a,1], Sishang Zhang[a,2], Zhangqian Wang[a,b,*], Feng Xu [c,d,*], Wenyi Zhong[a], Yizhou Liu[a], Xingxing Dong[a], Yi He[a]

[a] School of Modern Industry for Selenium Science and Engineering, Wuhan Polytechnic University, Wuhan, Hubei, 430023, China

[b] Hubei Key Laboratory of Industry Microbiology, Hubei University of Technology, Wuhan, Hubei, 430068, China

[c] College of Horticulture and Gardening, Yangtze University, Jingzhou 434025, China

[d] Engineering Research Center of Ecology and Agricultural Use of Wetland of Ministry of Education, Yangtze University, Jingzhou 434025, Hubei, China

[*] Corresponding author. *E-mail address*: wzqsnu@whpu.edu.cn (Zhangqian Wang), xufeng@yangtzeu.edu.cn (Feng Xu).Equal contribution.

Abstract

Background: Bostrycin, an anthraquinone secondary metabolite produced by *Nigrospora sphaerica*, exhibits broad-spectrum antitumor and antimicrobial activities, but its low production limits further development and application. Calcium ions (Ca^{2+}) are important intracellular signaling molecules that regulate fungal physiology and secondary metabolism, but their role in bostrycin biosynthesis remains unclear. This study aimed to investigate the effect of exogenous Ca^{2+} on bostrycin production and to elucidate the underlying molecular response using transcriptomic analysis.

Methods: Ca^{2+}, Mg^{2+}, Na^{+}, and K^{+} (supplemented as chloride salts) were screened for their ability to promote bostrycin production in *N. sphaerica* HCH285. The optimal Ca^{2+} concentration and addition time were determined by measuring bostrycin production using HPLC. Biomass accumulation, sporulation capacity, and extracellular nucleic acid and protein leakage were evaluated to characterize the physiological effects of Ca^{2+} treatment.Control and Ca^{2+}-treated cultures were subjected to transcriptome sequencing, followed by GO and KEGG enrichment analyses and qRT-PCR validation.

Results: Among all tested metal ions, Ca^{2+} showed the strongest stimulatory effect on bostrycin biosynthesis, with 4 g/L Ca^{2+} producing the highest yield of bostrycin with 63.6 ± 0.31 μg/mL, representing a 2.55-fold increase over the control. Ca^{2+} supplementation also significantly increased fungal biomass and sporulation capacity, suggesting that enhanced growth contributed to the elevated metabolite production. Increased extracellular nucleic acid and protein contents indicated altered cell integrity or secretion activity following Ca^{2+} treatment.Transcriptomic analysis identified DEGs most significantly enriched in metabolic pathways, including oxidative phosphorylation, while genes related to polyketide metabolism and ubiquinone biosynthesis were also annotated. Several genes associated with ion transport, energy metabolism, and secondary metabolite biosynthesis were significantly

upregulated. Among them, wbpA, talA, cho1, and aroB were further validated by qRT-PCR, indicating that Ca^{2+} supplementation triggered broad metabolic reprogramming associated with bostrycin accumulation.

Conclusions: Exogenous Ca^{2+} effectively enhances bostrycin production in *N. sphaerica* HCH285 through coordinated physiological and transcriptional responses. Transcriptomic analysis suggests that Ca^{2+} supplementation promotes energy metabolism, ion transport, and secondary metabolic processes associated with bostrycin biosynthesis. These findings provide new insights into calcium-mediated regulation of fungal secondary metabolism and offer a potential strategy for improving bostrycin production through fermentation optimization and metabolic engineering.

Keywords: *Nigrospora sphaerica*; Bostrycin; Calcium signaling; Transcriptomics; Oxidative phosphorylation

1 Introduction

Natural products encompass a diverse array of chemical components derived from animals, plants, and microorganisms, and have become one of the important sources of drugs or lead compounds for the treatment of major diseases [1]. These compounds exhibit significant physiological functionalities and have laid a solid foundation for modern pharmaceutical development. For example, synthesized endogenously in animals, play essential roles in regulating blood glucose homeostasis [2]. Similarly, quinidine isolated from the bark of the *Cinchona calisaya*, demonstrates potent antiarrhythmic activity [3]. With the deepening exploration of natural products, microbial sources of natural products have also yielded encouraging results.. Notable examples include streptomycin, obtained from the secondary metabolites of Actinobacteria such as *Streptomyces griseus* [4]; bacitracin, derived from the secondary metabolites of *Bacillus subtilis* [5]; penicillin, discovered in *Penicillium* [6]; and cephamycin, isolated from *Cephalosporium* [7]. From plants and animals to microorganisms, the remarkable diversity of natural product sources, coupled with their intrinsic unique bioactivities, has established a robust foundation for modern pharmaceutical development and promoted progressive advancements in related research fields.

However, as the demand for natural products continues to increase, their production capacity has struggled to meet market requirements, presenting a substantial challenge that constrains their further development and application. At present, natural products are primarily produced via total chemical synthesis, direct extraction from biological sources, and microbial synthesis [8, 9, 10]. The chemical synthesis approach is plagued by complex processes, high costs, and substantial environmental burdens. Direct extraction remains constrained by the limited availability of biological resources. In contrast, microbial synthesis exhibits distinct advantages over the aforementioned methods, including

environmental sustainability and low cost [11].

Bostrycin, an anthraquinone type natural product,was first discovered as a red pigment produced by Bostrychonema alpestre in 1968, has garnered significant attention due to its broad-spectrum anticancer, and antibacterial activities [12]. Studies demonstrate its potent inhibitory effects against diverse cancer cell lines, including breast, lung, liver, and colon cancers [13], as well as multifunctional bioactivities[14]. These attributes underscore its substantial potential for novel drug development. However, conventional methods for bostrycin production face critical limitations: chemical synthesis necessitates the construction of intricate anthraquinone scaffolds through laborious steps with low yields, while biosynthesis—though achieved using the endophytic fungal strain *Nigrospora sphaerica* HCH285 isolated from Artemisia argyi—yields only 28.23 μg of bostrycin per gram of extract [15], falling short of the thresholds required for research or clinical applications. Therefore, exploring efficient regulatory strategies to promote bostrycin accumulation via microbial biosynthesis holds substantial research value.

The biosynthesis of fungal secondary metabolites is accomplished through the coordinated interplay of multiple pathways, with their regulatory networks exhibiting profound complexity that involves multilevel signal transduction and gene expression regulation [16]. Studies have shown that that metal ions, acting as critical environmental signaling molecules, exert bidirectional regulatory effects (positive or negative) on fungal growth, reproduction, and secondary metabolite biosynthesis, demonstrating their deep involvement in the biosynthetic regulation of these compounds [17, 18]. Among these ions, calcium ion (Ca^{2+}), a physiologically active divalent cation, plays a pivotal role in fungal adaptation to environmental perturbations. Upon exposure to external stimuli, intracellular Ca^{2+} concentrations undergo dynamic fluctuations, which are subsequently transduced into

calcium-mediated signaling cascades to modulate diverse cellular processes, enabling fungi to adapt to environmental challenges [19, 20]. The regulatory role of Ca^{2+} in microbial secondary metabolite biosynthesis has been documented in prior studies.. Additionally, calcineurin [21] has been implicated in the regulation of ganoderic acid synthesis in *Agaricomycetes* cells [22]. However, reports on calcium signaling-mediated regulation of secondary metabolite biosynthesis in fungi remain scarce. Whether Ca^{2+} exerts regulatory effects during bostrycin biosynthesis remains unresolved and warrants further investigation. In this study, Ca^{2+} was identified from a panel of exogenous metal ions as a potent enhancer of bostrycin production in HCH285. The optimal supplementation conditions for Ca^{2+} were determined, followed by an characterization of bostrycin's cytotoxic effects on two cancer cell lines. Finally, transcriptomic analysis was performed to profile the global transcriptional changes associated with Ca^{2+} treatment, providing a basis for understanding the cellular response of *N. sphaerica* HCH285 to calcium supplementation.

2 Materials and methods

2.1 Materials and Chemicals

Artemisia argyi cv. Qiai was collected in October 2013 in Qichun County, Hubei Province, China, and *Nigrospora sphaerica* HCH285 was isolated from the rhizomes of these plants. The strain has since been maintained in our laboratory culture collection as a glycerol stock at −80 °C, and this preserved strain was used for all experiments reported in this study. Glucose, calcium chloride and ethyl acetate were purchased from SCR Company (Shanghai, China). Chromatographic grade methanol was obtained from Aladdin (Shanghai, China). Bostrycin standard products were purchased from MCE Company (Shanghai, China). $CaCl_2$, $MgCl_2$, NaCl, and KCl (analytical grade) were purchased from Sinopharm Chemical Reagent Co., Ltd. (Shanghai, China). PrimeScript™ RT Reagent Kit was purchased from Takara (Japan). Caco-2 and HeLa cells were obtained from the Cell Bank of the Chinese Academy of Sciences (Shanghai, China). The CCK-8 assay kit was purchased from Shanghai Beyotime Bio-Technology Co., Ltd. (Shanghai, China). The plant material was obtained from cultivated plants; *A. argyi* is neither a nationally protected plant species nor listed in the CITES Appendices, and all procedures followed national regulations and institutional guidelines. Therefore, no collection permit was required.

2.2 Activation and subculturing of strains

The frozen stock of *N. sphaerica* HCH285 was thawed, and 100 μL of the suspension was transferred onto PDA medium and incubated it at 28℃ for 5 days. A 1 cm diameter plug was aseptically excised from a solid culture of *N. sphaerica* HCH285 using a sterile punch and subsequently inoculated onto a fresh PDA plate.The inoculated plate was incubated at 28 °C for 5 days, and this subculturing procedure was repeated three times before use in experiments.

2.3 Extraction and content determination of bostrycin

Fermentation broth was collected and filtered through sterile cheesecloth to remove biomass, extract the supernatant twice with an equal volume of ethyl acetate, and then evaporate the ethyl acetate using a rotary evaporator. Dissolve the ethyl acetate extract of the fermentation broth in methanol and dilute it to a concentration of 500 μg/mL. The content of bostrycin in the fermentation broth was detected using HPLC [23]. Chromatographic separation was performed on an Elit C18 reversed-phase column (4.6 × 250 mm) with a mobile phase consisting of methanol and 0.3% formic acid (65:35, v/v) at a flow rate of 0.8 mL/min. The injection volume was 10 μL, the detection wavelength was set at 302 nm, and the total detection time was 10 min [24].

2.4 Screening for exogenous metal ions promoting bostrycin production in *N. sphaerica* HCH285

In order to screen out exogenous metal ions that can promote the biosynthesis of bostrycin in HCH285, the activated *N. sphaerica* HCH285 strain was inoculated into potato dextrose broth (PDB) medium and incubated under shaking conditions (28℃, 200 r/min) for 2 days to prepare the seed culture. Subsequently, the seed culture was transferred to PDB medium supplemented with various types and concentrations of exogenous metal chlorides, using an inoculum volume of 1% (v/v). Fermentation was conducted at a temperature of 25℃ and a shaking speed of 200 r/min for a duration of 3 days. Following this period, the bostrycin content was quantified using HPLC analysis.

2.5 Optimal Ca^{2+} supplementation

N. sphaerica HCH285 was inoculated into PDB medium supplemented with Ca^{2+} at concentrations of 1-10 g/L. After fermentation, secondary metabolites were extracted and their contents were determined to identify the optimal Ca^{2+} concentration.

N. sphaerica HCH285 was inoculated into PDB medium. Ca^{2+} was supplemented at 0, 12, 24, 36,

and 48 hours in the fermentation broth, and then the culture was continued in a constant-temperature shaking incubator for 72 hours. Secondary metabolites were extracted from the culture, and the bostrycin content was measured to determine the optimal timing for Ca^{2+} addition.

2.6 Spore production capacity measurement

The fungal blocks were extracted from the plates of *N. sphaerica* HCH285 and transferred to PDA medium containing 1-10 g/L Ca^{2+} respectively for 7 days of culture. Subsequently, spores were eluted from the culture using sterile water, serially diluted, and quantified via hemocytometer counting to determine the spore count per plate. Following spore enumeration, the agar medium was melted in a boiling water bath and filtered while hot to collect mycelial biomass. The harvested mycelia were dried to constant weight at 50°C, and the dry weight was recorded. The sporulation capacity of the fungus was evaluated as the number of spores produced per gram of dried mycelia.The dry weight of the mycelium was calculated as Dry weight of mycelium = (Weight of filter paper + dry mycelium) − Weight of filter paper [25]. The sporulation capacity of the fungus was evaluated as the number of spores produced per gram of dried mycelia, calculated using the formula as Sporulation capacity (spores/g) = (Spore concentration (spores/mL) × Total volume of spore suspension (mL)) / Dry weight of mycelium (g) [26].

2.7 Measurement of extracellular nucleic acid and protein leakage

To evaluate cellular integrity, the leakage of nucleic acids and proteins into the culture supernatant was monitored by measuring OD_{260} and OD_{280}, following previously described procedures [27, 28] with minor modifications. *N. sphaerica* HCH285 was grown in PDB medium until visible mycelial development. The culture was centrifuged at 5000 r/min for 5 min, the supernatant was discarded, and the mycelial pellet was collected. The mycelium was rinsed twice with sterile water, and 2 g (wet

weight) was transferred to 20 mL of fresh PDB medium either with or without 4 g/L Ca^{2+} (the optimal concentration determined in Section 2.5. Cultures were returned to the shaker (25 °C, 200 r/min). Samples were taken at 12, 24, 36, 48, 60, and 72 h, and the absorbance of the cell-free supernatant was measured at 260 nm and 280 nm using a spectrophotometer. Three independent biological replicates were analyzed for each time point.

2.8 Transcriptome analysis

2.8.1 Extraction of total RNA

N. sphaerica HCH285 was cultured in PDB medium containing Ca^{2+} for 72 hours (Ca^{2+} concentrations of 0 and 4 g/L). After fermentation, the mycelium was filtered through gauze, thoroughly washed with sterile water, and collected. Approximately 100 mg of mycelium was transferred to a pre-chilled mortar and ground into a fine powder under liquid nitrogen.Total RNA was extracted using Takara according to the manufacturer's instructions. Subsequently, 1 mL of RNA extraction reagent was added, and the mixture was further ground to ensure uniformity before being transferred to a 2 mL RNase-free microcentrifuge tube. Centrifuge at 4℃ at 13,000 r/min for 10 minutes, transfer the supernatant to a new RNase-free microcentrifuge tube, add 600 μL chloroform, and vigorously invert to mix. Centrifuge again at 13,000 r/min for 10 minutes. Transfer the upper layer to a new RNase-free microcentrifuge tube. Add 1/6 volume of isopropanol and 1/10 volume of sodium acetate, then incubate the mixture at -20℃ for 3 hours. Centrifuge at 13,000 r/min for 2 minutes and discard the supernatant. Wash the precipitate with 600 μL of ice-cold 70% ethanol, then centrifuge at 13,000 r/min for 2 minutes. Repeat this washing step three times. Allow the centrifuge tube to dry at room temperature to evaporate any residual ethanol. Finally, dissolve the precipitate in 30 μL of RNAase-free ddH_2O and store at -80℃ for subsequent use.

2.8.2 Construction and analysis of cDNA libraries

Following quality control verification of the RNA samples, eukaryotic mRNA was enriched using Oligo (dT)-conjugated magnetic beads. The purified mRNA was then subjected to random fragmentation buffer incubation with fragmentation buffer. First-strand cDNA synthesis was performed using random hexamer primers with fragmented mRNA as the template. Second-strand cDNA synthesis was subsequently carried out by adding reaction buffer, dNTPs, and DNA polymerase I. The double-stranded cDNA was purified using AMPure XP beads to remove residual enzymes and primers. The purified double-stranded cDNA was then subjected to end repair, an A tail was added and the sequencing connector was connected. Size selection of the adapter-ligated cDNA fragments was achieved using AMPure XP beads to retain fragments within the desired size range. Finally, perform PCR enrichment to obtain the final cDNA library.The PCR program was as follows: initial denaturation at 95 °C for 3 min; 15 cycles of 95 °C for 15 s, 60 °C for 30 s, and 72 °C for 30 s; and a final extension at 72 °C for 5 min. Library quality and concentration were assessed using an Agilent Bioanalyzer 2100 (Agilent Technologies, USA).Following cDNA library construction, the library was sequenced by Zhongke Xinsheng Biotechnology Co., Ltd. (Shanghai, China) using second-generation sequencing (RNA-seq), with three biological replicates per sample.

2.8.3 Differential expression analysis and functional enrichment

To identify differentially expressed genes (DEGs) between the control and experimental groups, differential expression analysis was conducted using the DESeq2 package. Genes with an adjusted padj < 0.05 and an absolute $|\log_2 FC| > 1$ were defined as statistically significant DEGs, serving as the criteria for downstream functional enrichment and pathway analyses. Gene Ontology enrichment analysis was used to interpret the functional annotations of DEGs in biological processes, molecular

functions, and cellular components [29]. Pathway enrichment analysis based on the Kyoto Encyclopedia of Genes and Genomes revealed the core metabolic and signal transduction pathways involved in DEGs [30].

2.9 Real-time fluorescent quantitative PCR (qRT - PCR)

To validate the transcriptome data, four significantly upregulated DEGs were selected for qRT-PCR analysis. Total RNA was extracted as described in Section 2.9.1, and cDNA was synthesized using a PrimeScript™ RT Reagent Kit (Takara, Japan) following the manufacturer's instructions. qRT-PCR was performed using TB Green® Premix Ex Taq™ II (Takara, Japan) on a Bio-Rad CFX96 system. The GADPH gene was used as the internal reference. Primers were designed using Primer Premier 6.0 and are listed in Supplementary Table S1. The PCR cycling conditions were: 95 °C for 30 s; 40 cycles of 95 °C for 5 s and 60 °C for 30 s; followed by a melting curve analysis from 65 °C to 95 °C. Each reaction was performed in three technical replicates from three independent biological replicates. Relative expression levels were calculated using the $2^{-}\Delta\Delta C^{T}$ method [31].

2.10 Evaluation of the cytotoxic effects of bostrycin on cells

Both cell lines were cultured in DMEM supplemented with 10% fetal bovine serum at 37°C in a 5% CO_2 humidified incubator. After three subculturing cycles, the cells were seeded into 96-well plates at a density of 5×10^3 cells per well (200 μL medium per well) and incubated for 24 h. Subsequently, cells were exposed to different concentrations of bostrycin solution (0.1, 0.2, 0.4, 0.8, 1.6, 3.2, 6.4, 12.8, 25.6, and 51.2 μg/mL for 48 h) for 48 h. After removal of the medium, cell viability of Caco-2 and HeLa cells was determined according to the CCK-8 commercial reagent kit protocol.

2.11 Data processing and analysis

Data derived from three independent biological replicates are presented as mean ± standard

deviation. Data visualization and preliminary analyses were conducted using Origin 2024. For multiple-group comparisons, one-way analysis of variance was performed in SPSS 26, followed by Duncan's multiple range test for post-hoc analysis when statistical significance was detected ($P < 0.05$). For comparisons between two groups, independent samples t-test was employed to assess significance ($P < 0.05$).

3 Results

3.1 Screening for exogenous metal ions promoting bostrycin accumulation in *N. sphaerica* HCH285

To investigate the effects of exogenous metal ions on bostrycin biosynthesis in *N. sphaerica* HCH285, Ca^{2+}, Mg^{2+}, Na^{+}, and K^{+} (supplemented as chloride salts) at concentrations of 2, 4, and 6 g/L were added to PDB medium at the onset of fermentation.. Experimental results are shown in Fig. 1. Adding Ca^{2+} to the PDB medium at the beginning of *N. sphaerica* HCH285 fermentation can increase the yield of *N. sphaerica* HCH285 biosynthetic bostrycin. With the gradual increase of Ca^{2+} addition concentration, the yield of bostrycin shows a trend of increasing first and then decreasing. The optimal yield was achieved at 4 g/L Ca^{2+}, which was significantly higher than yields observed at 2 g/L and 6 g/L. In contrast, supplementation with Mg^{2+}, Na^{+}, or K^{+} at varying concentrations showed no significant impact on bostrycin biosynthesis, failing to enhance production.

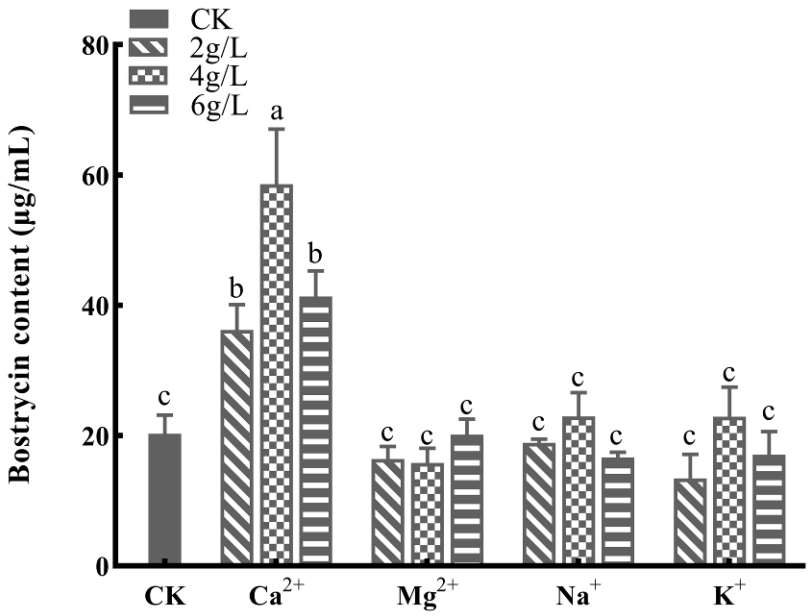


Fig. 1 The changes in the yield of bostrycin with different metal ions added

CK, control without metal ion supplementation.Value represent the mean ± standard deviation of

three independent replicates. Different letters indicate statistically significant differences among treatments ($P < 0.05$)

3.2 Optimization of Ca^{2+} concentration and addition time in bostrycin production

Adding exogenous Ca^{2+} to the fermentation medium can significantly enhance the bostrycin accumulation of *N. sphaerica* HCH285. In order to determine the optimal concentration of Ca^{2+} to increase the concentration, different concentrations of Ca^{2+} were added to the culture medium at the beginning of fermentation. Experimental results are summarized in Fig. 2. Bostrycin yield exhibited a biphasic response to increasing Ca^{2+} concentrations, initially rising and subsequently declining. At 4 g/L Ca^{2+}, the concentration reached 63.6 ± 0.3 μg/mL, compared to 24.9 ± 1.6 μg/mL in the control group, representing a 2.55 fold increase. While bostrycin production remained higher than the control at Ca^{2+} concentrations exceeding 4 g/L, the promoting effect gradually diminished with further increases in Ca^{2+} concentration. Based on these findings, the optimal concentration of exogenous Ca^{2+} addition is 4 g/L.

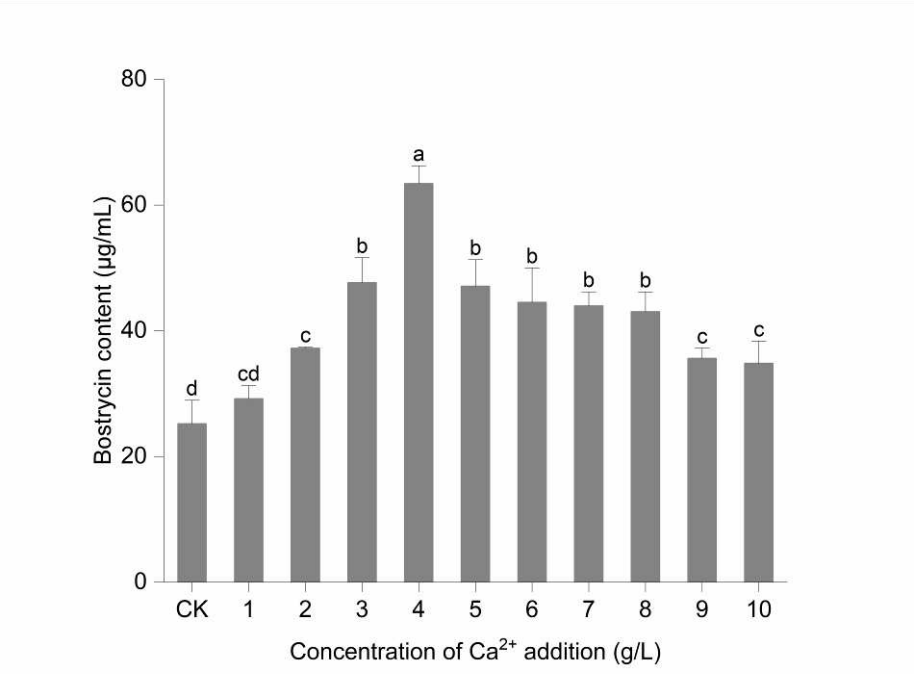


Fig. 2 The changes of bostrycin yield after the addition of different concentrations of Ca^{2+}

CK, control without Ca^{2+} supplementation.Values represent the mean ± standard deviation of three independent replicates. Different letters indicate statistically significant differences among treatments ($P < 0.05$)

To investigate the effects of Ca^{2+} supplementation timing on bostrycin accumulation in *N. sphaerica* HCH285, 4 g/L calcium chloride was added to the fermentation medium at different time intervals. The experimental results are shown in Fig. 3. The highest promoting effect on bostrycin accumulation was observed when Ca^{2+} was supplemented during the early fermentation phase of HCH285. In contrast, Ca^{2+} supplementation after 24 h of fermentation resulted in a significantly lower stimulatory effect compared to the early fermentation phase supplementation. We speculate that Ca^{2+} exerts a stronger regulatory role during the early fermentation phase than in the mid-to-late fermentation phases of *N. sphaerica* HCH285. Consequently, the yield of bostrycin obtained by adding Ca^{2+} at the initial stage of strain fermentation is higher than that obtained by adding Ca^{2+} in the middle and later stages of fermentation.

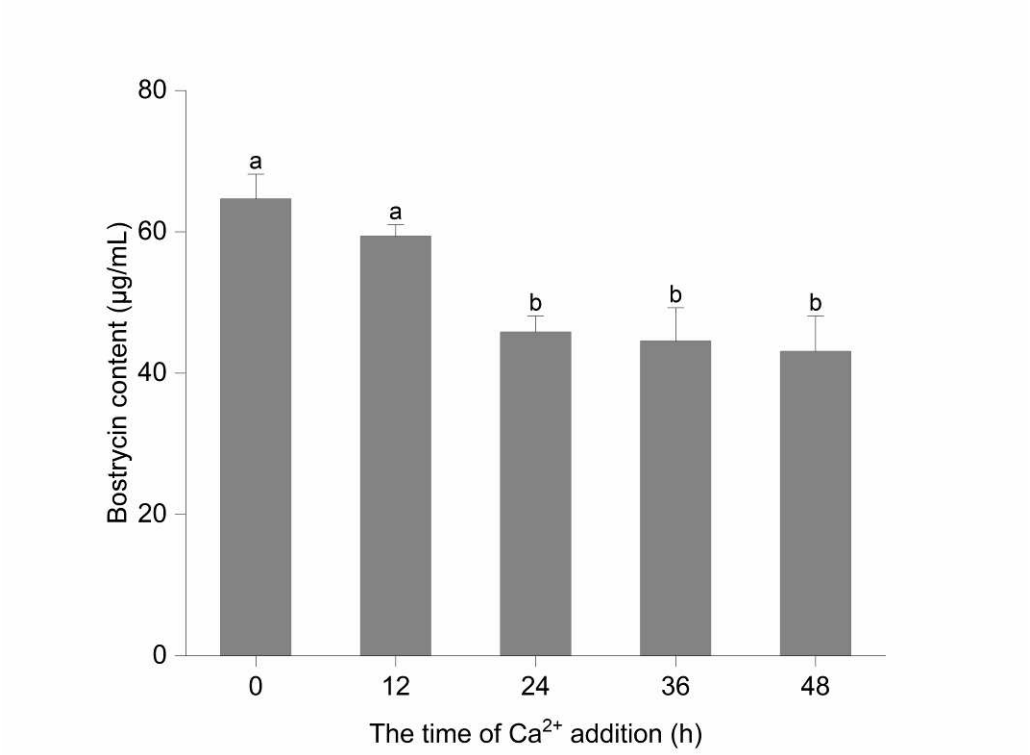


Fig. 3 The changes of bostrycin yield under different addition times of Ca^{2+}

Values represent the mean ± standard deviation of three independent replicates. Different letters indicate statistically significant differences among treatments ($P < 0.05$)

3.3 Enhanced Biomass Accumulation in *N. sphaerica* HCH285 by Ca^{2+} Supplementation

In order to study the effect of different concentrations of exogenous Ca^{2+} on the biomass of *N. sphaerica* HCH285, different concentrations of Ca^{2+} were added to the culture medium in the early stage of fermentation. As shown in Fig. 4, Ca^{2+} supplementation at concentrations of 4, 5, 6, and 7 g/L significantly enhanced the biomass of HCH285. In contrast, no significant impact on biomass was observed when Ca^{2+} concentrations were either below 4 g/L or exceeded 7 g/L. These results indicate a concentration-dependent stimulatory effect of Ca^{2+} on fungal growth within the optimal range of 4-7 g/L.

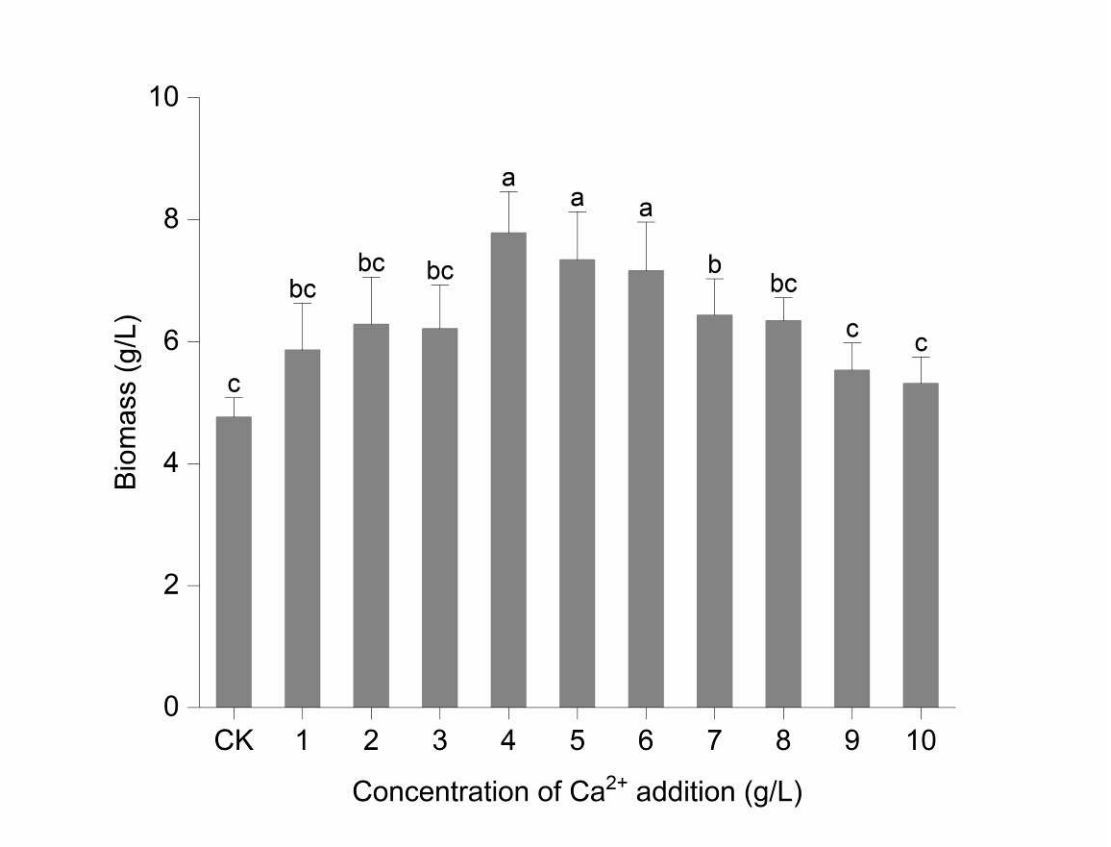


Fig. 4 The changes of strain biomass after the addition of different concentrations of Ca^{2+} CK, control without Ca^{2+} supplementation.Values represent the mean ± standard deviation of three independent replicates. Different letters indicate statistically significant differences among treatments ($P < 0.05$)

3.4 Enhanced sporulation capacity in *N. sphaerica* HCH285 by Ca^{2+} supplementation

To investigate the effects of exogenous Ca^{2+} supplementation at varying concentrations on the sporulation of *N. sphaerica* HCH285, different concentrations of Ca^{2+} were added to the fermentation medium. As shown in Fig. 5, Ca^{2+} supplementation significantly promoted spore production capacity in *N. sphaerica* HCH285, the results demonstrate that the spore formation of HCH285 reaches its peak within the range of 3-5 g/L Ca^{2+}.

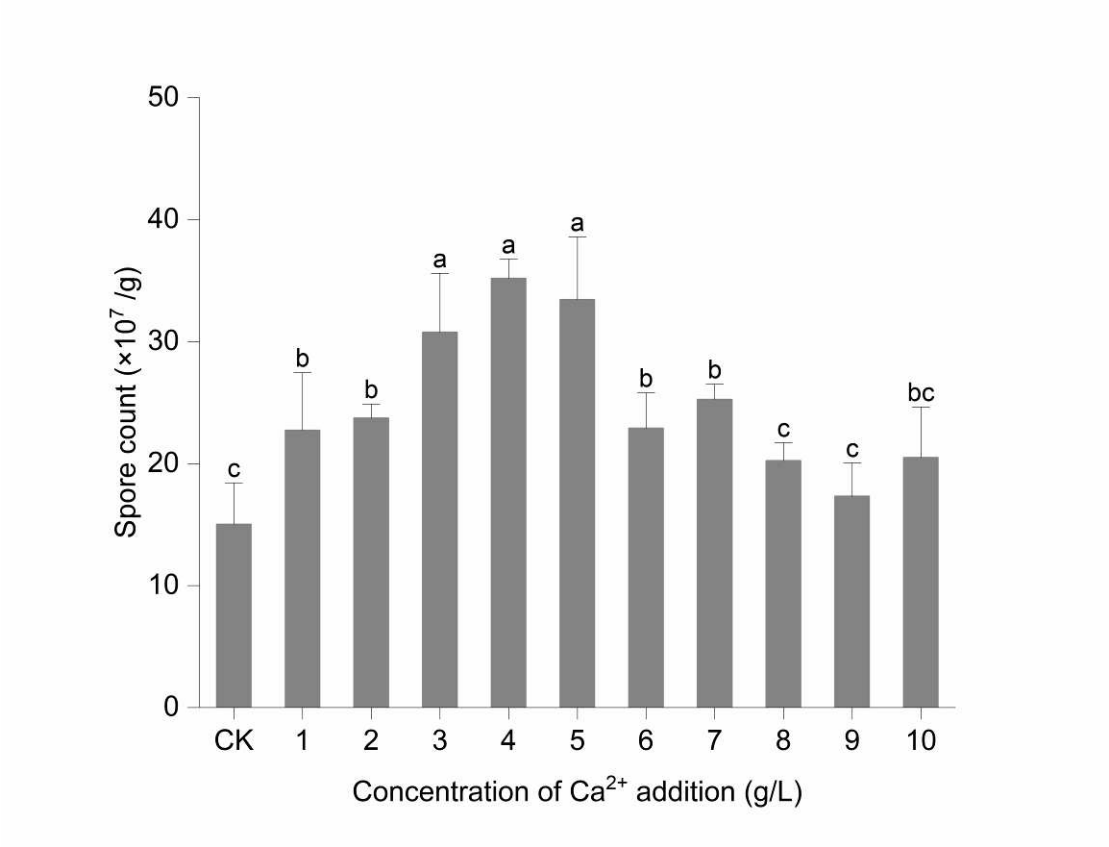


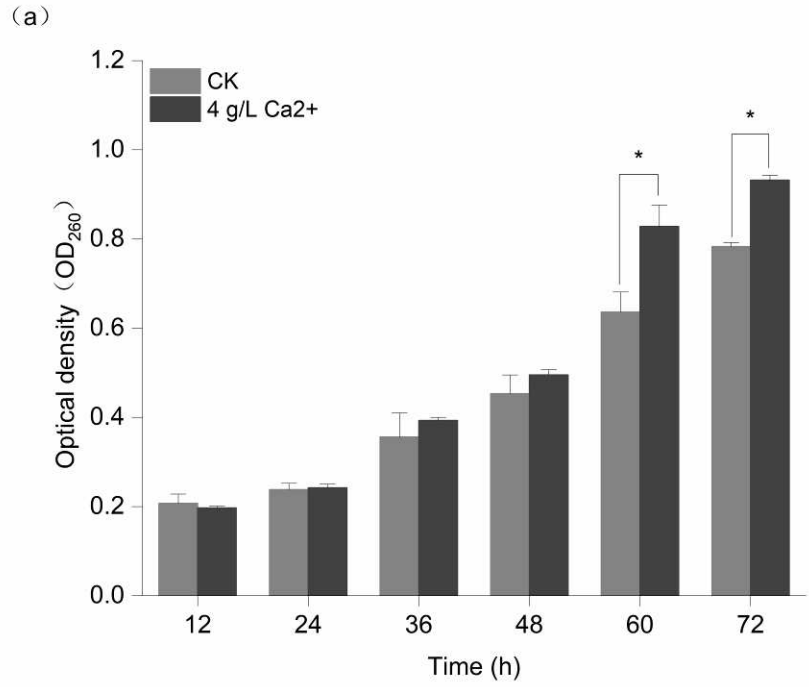
Fig. 5 The changes in the spore-forming ability of strains after the addition of different concentrations of Ca^{2+}

CK, control without Ca^{2+} supplementation. Values represent the mean ± standard deviation of three independent replicates. Different letters indicate statistically significant differences among treatments ($P < 0.05$)

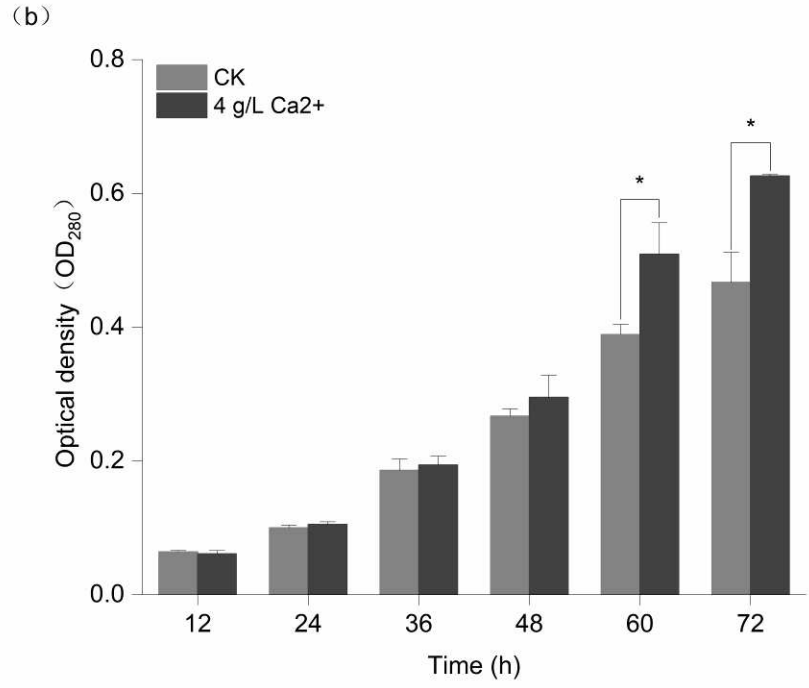
3.5 Extracellular nucleic acid and protein leakage

Previous studies have revealed that cell membrane permeability significantly influences extracellular pigment production, which can be assessed through protein exudation and nucleic acid leakage [32]. As shown in Fig. 6, the OD_{260} and OD_{280} values in the Ca^{2+}-supplemented group were significantly higher than those in the control group after 48 h of fermentation, demonstrating that Ca^{2+} modulates cell membrane permeability in *N. sphaerica* HCH285. This increase in permeability likely facilitates enhanced transport of bostrycin across the cell membrane into the fermentation broth,

thereby elevating its extracellular concentration. Several processes could contribute to this observation, including enhanced secretion, altered cell integrity, or increased autolysis. The present data do not distinguish among these possibilities, and thus the increased leakage should not be interpreted as direct evidence of altered membrane permeability.



328



329

330 **Fig. 6 Changes in the release of intracellular proteins (a) and nucleic acids (b) in *N. sphaerica***

331 **HCH285 after Ca^{2+} addition**

332 **Values represent the mean ± standard deviation of three independent replicates. Asterisks (*)**

333 **indicate statistically significant differences among treatments ($P < 0.05$)**

3.6 Transcriptome analysis

3.6.1 Quality analysis of transcriptome sequencing data

In this study, transcriptomic analysis was performed to investigate the molecular mechanism by which exogenous Ca^{2+} modulates the biosynthesis of the secondary metabolite bostrycin in *N. sphaerica* HCH285. RNA samples were extracted from fungal cultures treated with varying Ca^{2+} concentrations (0 and 4 g/L) and subjected to sequencing on the Illumina platform. Quality assessment of the sequencing data (*Additional File 1*) demonstrated that over 95% of bases achieved a Q20 score and over 90% reached Q30, with GC content exceeding 55% across all samples. These metrics confirm the high quality and reliability of the transcriptomic datasets, ensuring the validity of subsequent bioinformatic analyses.

3.6.2 Transcriptome functional annotation and screening results of significantly different genes

To comprehensively investigate gene functions, we conducted functional annotation of unigenes using five major databases: Nr, Pfam, Swiss-Prot, KEGG, and GO. As summarized in *Additional File 2*, only 3.14% of unigenes were annotated across all five databases, while 54.43% (14,589 sequences) were annotated in at least one database. Notably, metabolism-related genes exhibited significant enrichment in KEGG pathways (21.69% of annotated genes). Differential expression analysis identified 336 significantly regulated genes ($Log_2FC \geq 2$, $P < 0.05$) compared to the control group (Fig. 7). Among these, 282 genes were up-regulated and 54 genes were down-regulated, indicating a pronounced transcriptional response to Ca^{2+} treatment.

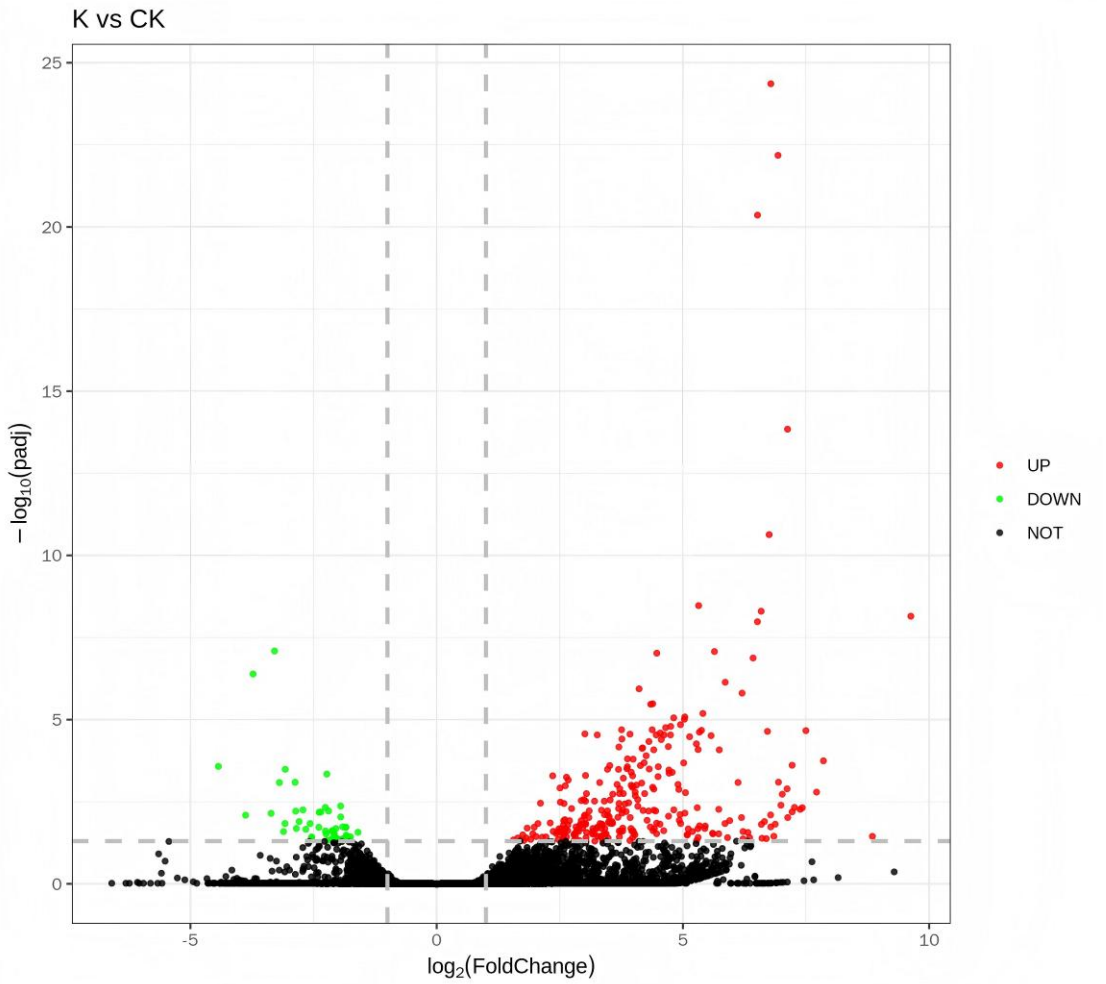
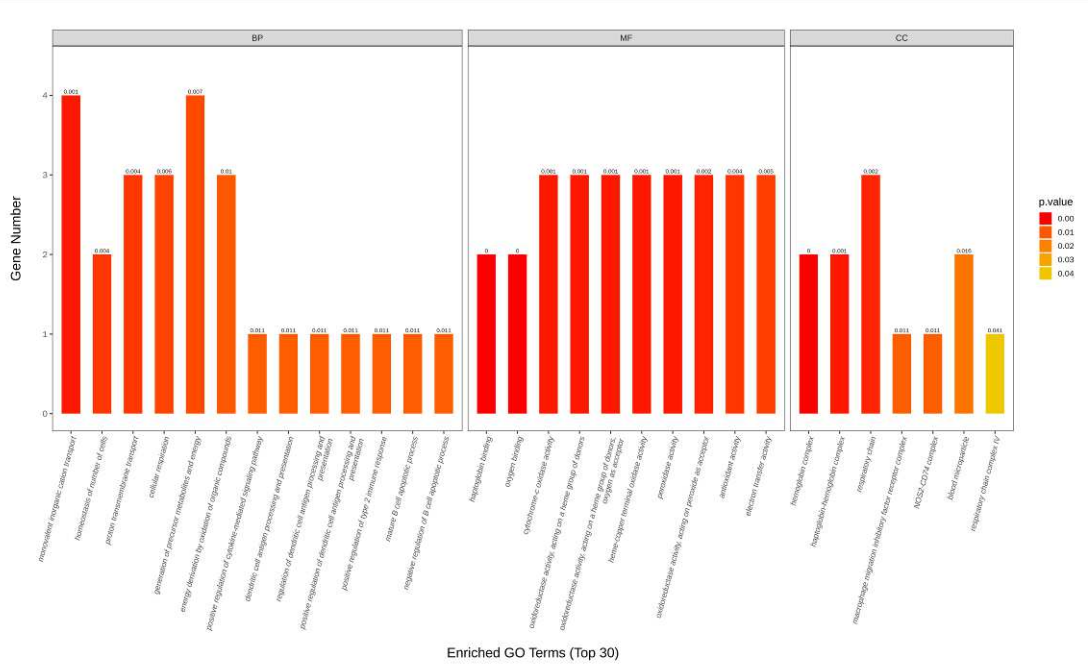


Fig. 7 Volcanic map of genes with significant differences

3.6.3 GO functional enrichment analysis of differentially expressed genes

To elucidate the functional classification of DEGs in *N. sphaerica* HCH285 under exogenous Ca^{2+} regulation, a systematic GO annotation was performed across three principal categories: Biological Process (BP), Cellular Component (CC), and Molecular Function (MF) (*Additional File 3*). The analysis uncovered distinct enrichment patterns, with metabolic processes (1,627 genes), cellular processes (1,496 genes), and response to stimuli (409 genes) being significantly overrepresented in BP. For MF, catalytic activity (1,473 genes), binding (1,300 genes), and transporter activity (188 genes) constituted the predominant functional classes. In CC annotations, genes were predominantly localized to the cell membrane (1,085 genes) and organelles (1,069 genes). Furthermore, subsequent enrichment

analysis identified the top 30 significantly enriched GO terms (Fig. 8). The enrichment analysis revealed a hierarchical pattern of functional categories based on significance. The most significantly enriched terms included monovalent inorganic cation transporter, generation of precursor metabolites and energy, cation transport, extracellular exosome, and extracellular organelle. These were followed by moderately enriched terms such as proton transmembrane transport, cellular respiration, energy derivation by oxidation of organic compounds, inorganic cation transmembrane transport, inorganic ion transmembrane transport, and cation transmembrane transport. Subsequent enrichment tiers featured homeostasis of cell number, haptoglobin binding, oxygen binding, hemoglobin complex, haptoglobin-hemoglobin complex, and blood microparticle. The least enriched terms included macrophage migration inhibitory factor receptor complex, NOS2-CD74 complex, respiratory chain complex IV, and MHC class II protein complex. Significant enrichment of pathways related to the generation of precursor metabolites and energy and cellular respiration suggests that Ca^{2+} may enhance mitochondrial oxidative phosphorylation efficiency, thereby elevating ATP synthesis to meet the high energy demands of secondary metabolism. This inference is further supported by KEGG enrichment analysis, in which thermogenesis and oxidative phosphorylation were among the most significantly enriched pathways. [33].



380

381 **Fig. 8 Shows the GO enrichment analysis results of genes with significant differences between the**

382 **calcium ion addition treatment group and the non-calcium ion addition treatment group**

383 **3.6.4 KEGG functional enrichment analysis of differentially expressed genes**

384 The KEGG Pathway database encompasses five major categories: Metabolism, Genetic

385 Information Processing, Environmental Information Processing, Cellular Processes, and Organismal

386 Systems. KEGG enrichment analysis of DEGs under Ca^{2+} treatment was conducted to explore the

387 potential mechanisms by which Ca^{2+} promotes bostrycin biosynthesis in *N. sphaerica* HCH285. Fig. 9

388 displays the top 20 most significantly enriched pathways for up - regulated DEGs ($P < 0.05$). The most

389 enriched pathway was metabolic pathways, followed by thermogenesis, oxidative phosphorylation, and

390 cardiac muscle contraction. Pathways such as arachidonic acid metabolism and ribosome biogenesis in

391 eukaryotes exhibited moderate enrichment, while pathways like regulation of lipolysis in adipocytes,

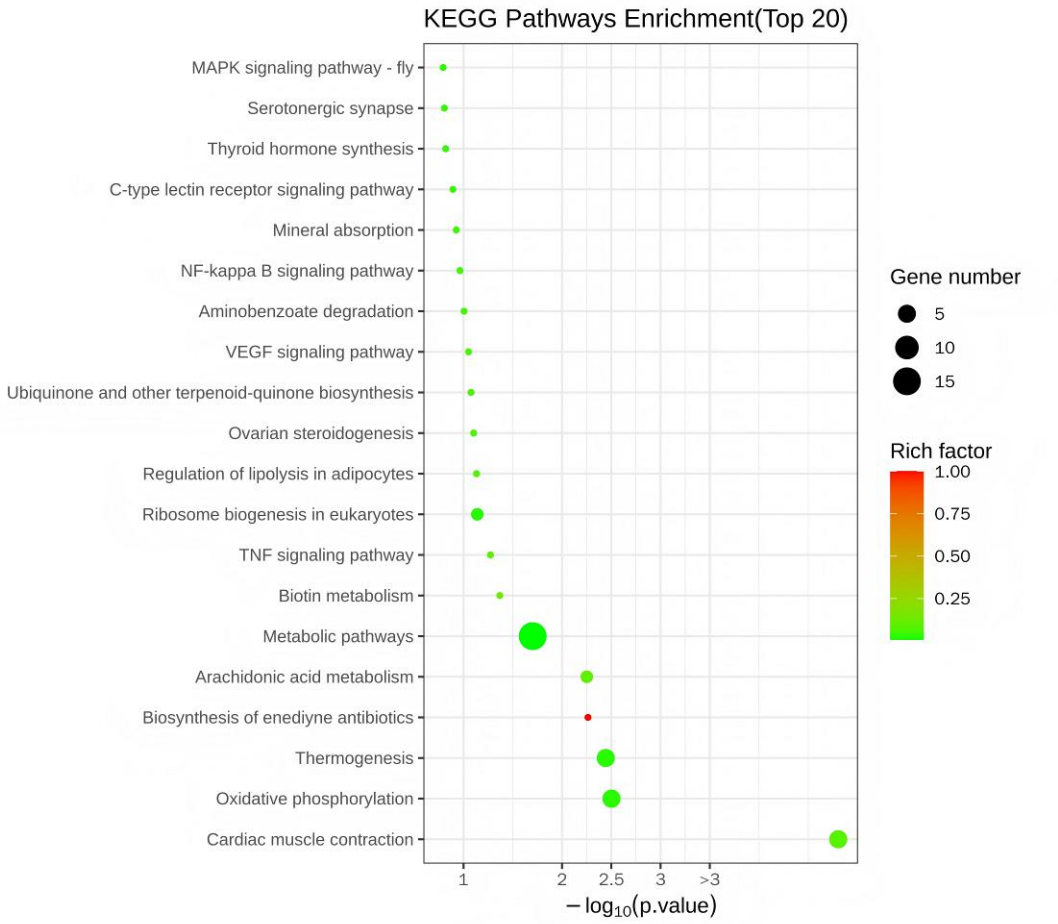
392 biotin metabolism, biosynthesis of enediyne antibiotics, and uubiquinone and other terpenoid-quinone

393 biosynthesis showed minimal enrichment (1 - 2 DEGs). Fig. 10 illustrates the top 20 enriched pathways

394 for down - regulated DEGs ($P < 0.05$), predominantly in metabolic pathways, with pathways such as

biosynthesis of secondary metabolites, sesquiterpenoid and triterpenoid biosynthesis, and pentose and glucuronate interconversions exhibiting only 1 - 2 enriched DEGs.

The broad enrichment of Metabolic pathways suggests that Ca^{2+} facilitates the biosynthesis of bostrycin by activating precursor-supplying pathways such as arachidonic acid metabolism. Specifically, the enrichment of the biosynthesis of enediyne antibiotics pathway directly correlates with bostrycin synthesis, likely through the activation of polyketide synthase gene clusters. Conversely, the downregulation of competing pathways, such as sesquiterpenoid and triterpenoid biosynthesis and pentose and glucuronate interconversions, indicates a metabolic reallocation of resources toward bostrycin production under Ca^{2+} treatment. Energy metabolism pathways, including oxidative phosphorylation and thermogenesis, were significantly upregulated, implying that Ca^{2+} enhances mitochondrial respiratory chain activity (such as complexes I - IV) to boost ATP synthesis, thereby meeting the high energy demands of polyketide biosynthesis. The activation of thermogenesis may further mitigate oxidative stress by regulating proton gradients via uncoupling proteins, ensuring a steady supply of reducing equivalents (NADH/NADPH) for polyketide chain elongation. In summary, Ca^{2+} directly activates the biosynthesis of enediyne antibiotics pathway, supporting bostrycin production through energy optimization and redox regulation, thereby laying the foundation for Ca^{2+}-mediated metabolic engineering strategies in fungal natural product biosynthesis.



412

413 **Fig. 9 Results of KEGG enrichment analysis of up-regulated DEGs between the Ca^{2+} -treated and**

414 **non-treated groups**

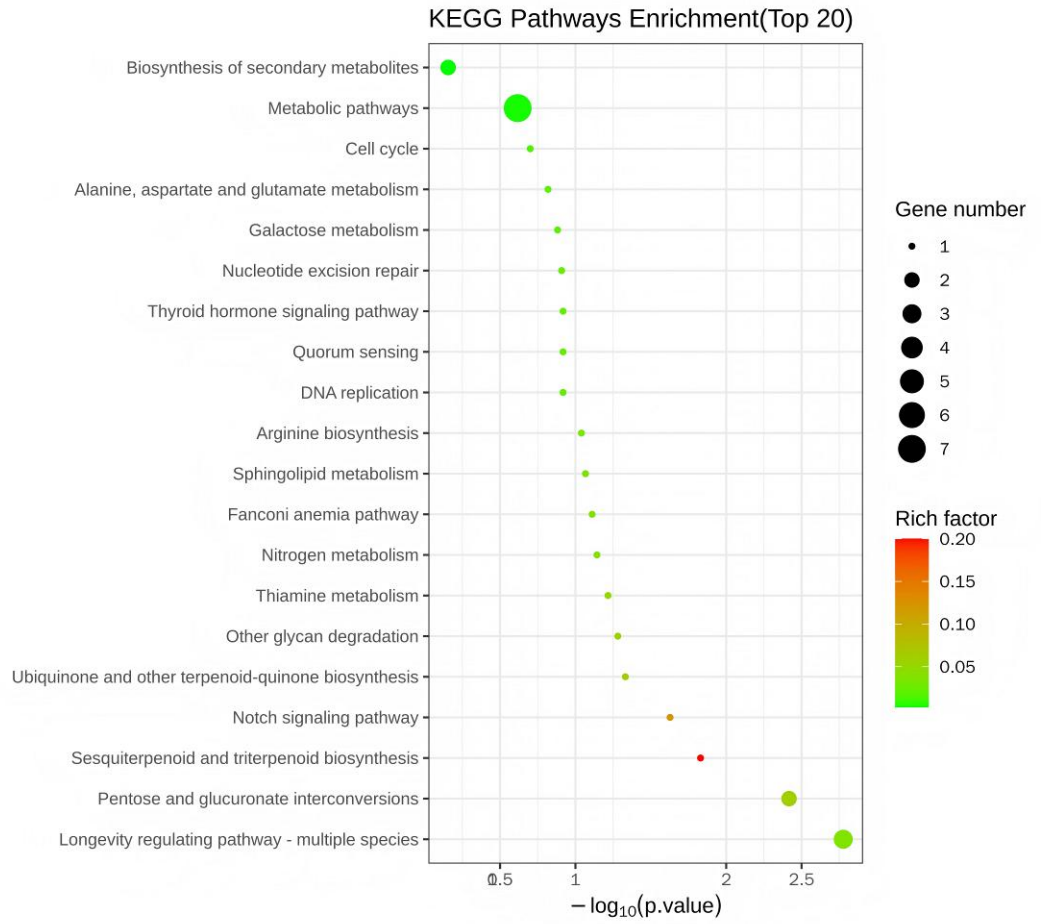
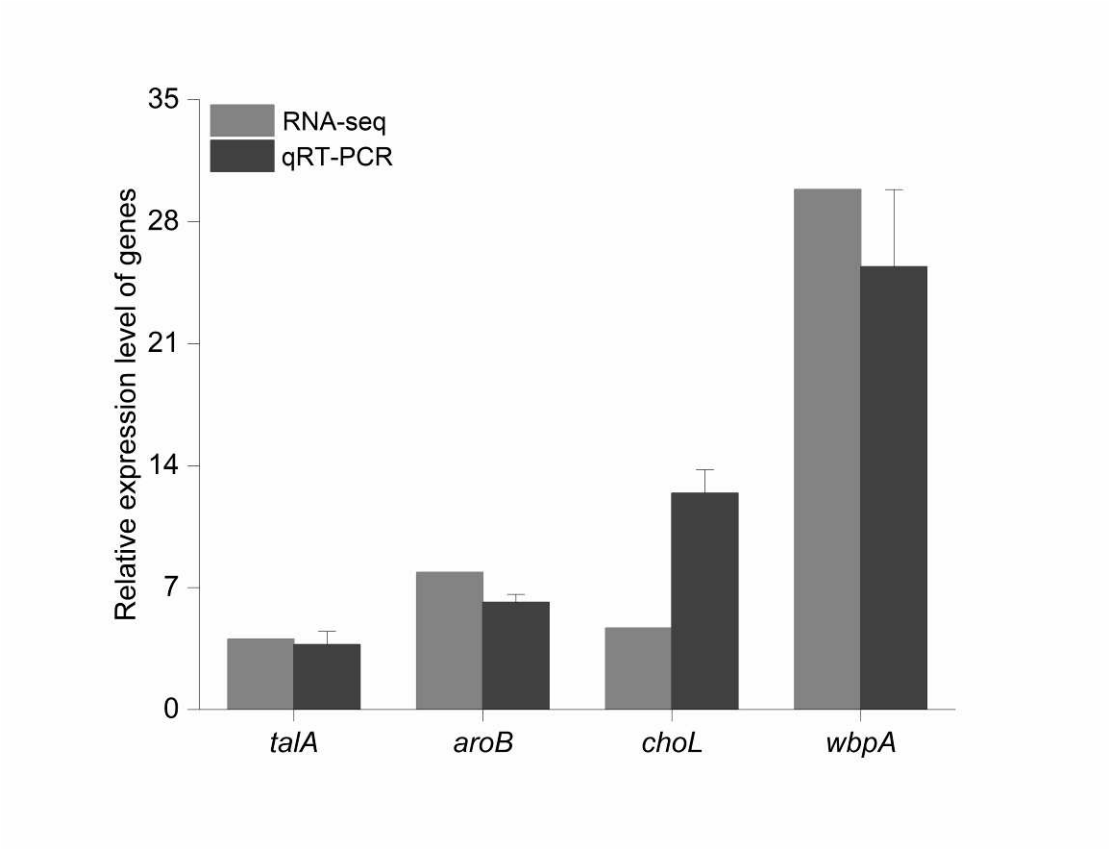


Fig. 10 Results of KEGG enrichment analysis of down-regulated DEGs between the Ca^{2+} -treated and non-treated groups

3.6.5 Verification results of real-time fluorescent quantitative PCR (qRT – PCR)

As shown in Fig. 11, qRT - PCR analysis demonstrated that the expression levels of four DEGs were significantly up-regulated following exogenous Ca^{2+} supplementation compared to the control group. These results align closely with transcriptome sequencing data, thereby validating the reliability of the transcriptomic findings.



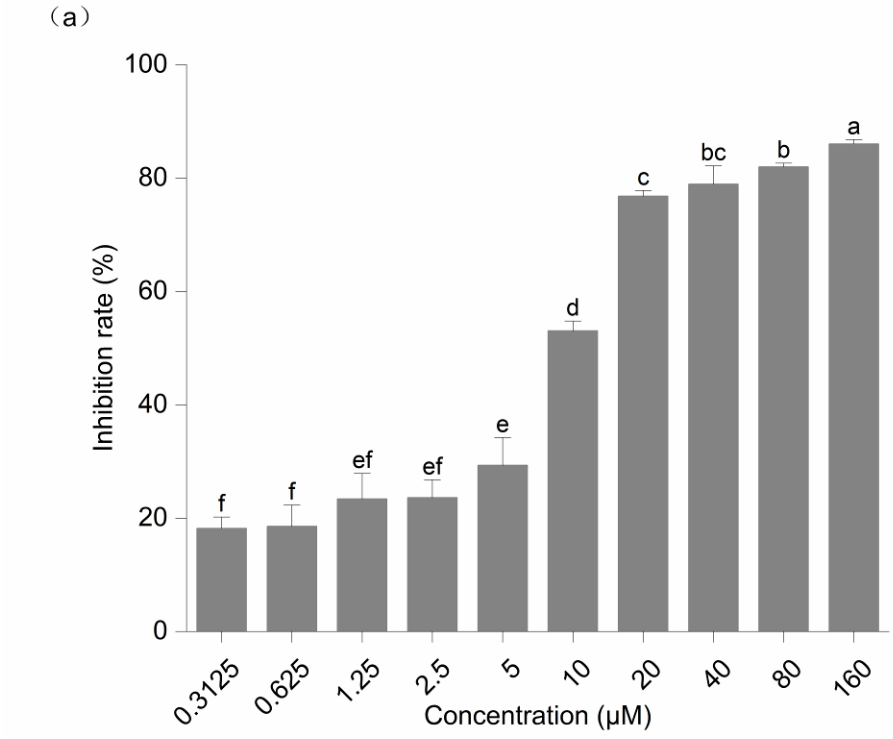
423

424 **Fig. 11 Comparison results of relative expression of candidate genes by RNA-seq**

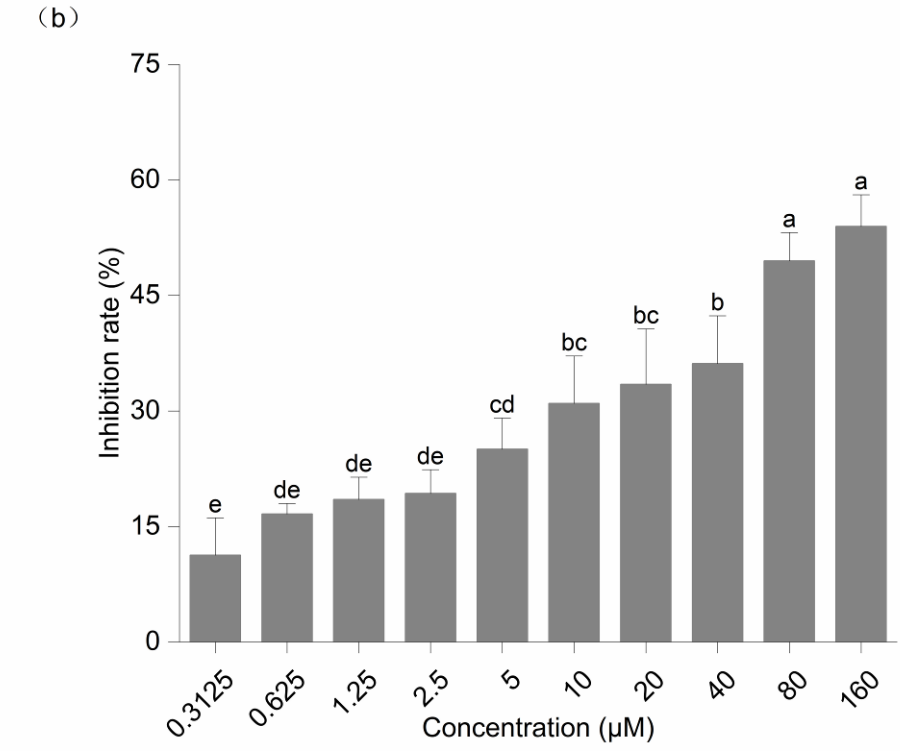
425 **and qRT-PCR under Ca^{2+} treatment**

426 **3.7 Evaluation of the cytotoxic effects of bostrycin on cells**

427 Caco-2 and HeLa cells were exposed to different concentrations of bostrycin to assess its
428 cytotoxic effects. Concentration-dependent inhibition of cell proliferation was observed in both cell
429 lines following bostrycin exposure (Fig. 12). The half-maximal inhibitory concentration for Caco-2
430 cells was determined to be 2.0 μg/mL, with an 80% suppression rate achieved at 26.9 μg/mL. In
431 contrast, HeLa cells exhibited weak cytotoxic response to bostrycin treatment, demonstrating merely
432 54% inhibition even at 53.8 μg/mL. Comparative analysis thus revealed significantly greater
433 susceptibility of Caco-2 cells to bostrycin-mediated growth inhibition relative to HeLa cells.



434



435

436 **Fig. 12 Inhibition rates of bostrycin on Caco-2 (a) and HeLa (b) cell**

437 **Values represent the mean ± standard deviation of three independent replicates. Different letters**

438 **indicate statistically significant differences among treatments (P < 0.05)**

4 Discussion

Metal ions play a critical role in microbial growth, metabolism, and reproduction [34]. Current studies have demonstrated that cationic metal ions such as Ca^{2+}, Na^{+}, and Mg^{2+} regulate multiple biological processes in filamentous fungi, including secondary metabolite biosynthesis and mycelial growth, through pathways such as signal transduction modulation. To identify a method for enhancing bostrycin biosynthesis in *N. sphaerica* HCH285, it was inoculated into media supplemented with exogenous metal ions of varying types, followed by analysis of bostrycin content. The results revealed that exogenous Ca^{2+} supplementation significantly increased yield of bostrycin in the fermentation broth. Prior studies have reported that exogenous supplementation of Ca^{2+} enhances the production yield of hypocrellins, perylenequinone compound, in the filamentous fungus *Shiraia sp.* Slf14 [32]. The quinone compound bostrycin is structurally similar to hypocrellins [33], and our research results further confirm that Ca^{2+} can regulate the biosynthesis of bostrycin in *N. sphaerica* HCH285. However, the enhancement of the yield of bostrycin mediated by Ca^{2+} shows a non-concentration-dependent relationship: The stimulating effect tends to stabilize and reach the maximum at a specific concentration. Beyond this concentration, a further increase in the concentration of Ca^{2+} will reduce the promoting effect. In this study, the optimal Ca^{2+} concentration was determined to be 4 g/L, yielding a bostrycin content approximately 2.55 fold higher than the control group, indicating that 4 g/L represents the most effective supplementation level. Furthermore, studies have found that when exogenous metal ions are added at different growth stages of filamentous fungi, the regulatory effects of metal ions on filamentous fungi are different. This study investigated the impact of Ca^{2+} supplementation timing on bostrycin biosynthesis in *N. sphaerica* HCH285. The results demonstrated that Ca^{2+} addition during the initial 0-12 h of fermentation significantly enhanced bostrycin yield

compared to supplementation after 12 h. Additionally, by examining the effects of varying Ca^{2+} concentrations on biomass and sporulation in *N. sphaerica* HCH285, we found that Ca^{2+} concentrations of 4, 5, and 6 g/L maximized both biomass accumulation and sporulation efficiency. Collectively, these findings demonstrate that exogenous Ca^{2+} supplementation exerts a multifaceted regulatory role in *N. sphaerica* HCH285, significantly promoting critical biological processes such as growth and sporulation. Previous studies have established that cell membrane permeability in filamentous fungi is a critical factor influencing extracellular pigment production [31, 33]. During pigment excretion, increased membrane permeability facilitates higher efficiency of pigment efflux [35]. To evaluate this mechanism, we compared membrane permeability changes between Ca^{2+} supplemented and non-supplemented groups. As evidenced by the experimental results, the total protein content and nucleic acid leakage in the Ca^{2+} supplemented group were significantly higher than those in the control group at 48 h of fermentation.The significantly higher OD values observed in Ca^{2+}-treated cultures after 48 h indicate increased extracellular nucleic acid and protein content. However, this observation alone does not constitute direct evidence of altered membrane permeability. Elevated extracellular nucleic acids and proteins can arise from multiple processes, including enhanced secretion, release of extracellular vesicles, autolysis, or cell lysis.

Previous experimental results confirmed that supplementation with 4 g/L Ca^{2+} in the culture medium enhances bostrycin biosynthesis in *N. sphaerica* HCH285. To preliminarily elucidate the molecular mechanisms underlying Ca^{2+} mediated regulation of bostrycin production, transcriptome sequencing was performed on strains subjected to either Ca^{2+} free treatment or 4 g/L Ca^{2+} supplementation, followed by transcriptomic analysis. KEGG enrichment analysis revealed that DEGs were most significantly enriched in metabolic pathways, indicating substantial alterations in metabolic

activity under Ca^{2+} regulation in *N. sphaerica* HCH285. KEGG enrichment analysis revealed that DEGs were most significantly enriched in metabolic pathways, indicating that Ca^{2+} induces substantial metabolic reprogramming in HCH285. Notably, DEGs were also substantially enriched in pathways related to thermogenesis and oxidative phosphorylation. GO enrichment analysis further revealed that the most significantly enriched terms included monovalent inorganic cation transporter, generation of precursor metabolites and energy, cation transport, extracellular exosome, and extracellular organelle. These findings collectively suggest that Ca^{2+} regulates bostrycin biosynthesis by modulating metabolic flux, energy metabolism, and transmembrane transport processes in *N. sphaerica* HCH285. We speculate that Ca^{2+} enhances metabolic processes in *N. sphaerica* HCH285, thereby increasing metabolic activity. Concurrently, Ca^{2+} significantly regulates energy-generating processes such as thermogenesis and oxidative phosphorylation, ensuring sufficient energy supply to sustain heightened metabolic demands. This dual regulation amplifies the biosynthetic activity of bostrycin in *N. sphaerica* HCH285, ultimately leading to elevated bostrycin production.

These findings provide a foundation for further genetic improvement of *N. sphaerica* HCH285 to achieve higher bostrycin yields.

5 Conclusion

This study demonstrated that exogenous Ca^{2+} supplementation (at 4 g/L) significantly increased bostrycin accumulation in the fermentation broth of *N. sphaerica* HCH285, accompanied by enhanced biomass and sporulation. Transcriptomic profiling revealed that Ca^{2+} treatment was associated with transcriptional changes in energy metabolism and cation transport-related pathways. Additionally, bostrycin showed inhibitory activity against Caco-2 colon cancer cells. However, since yield of bostrycin were measured on a volumetric basis without normalization to biomass, the observed increase cannot be unequivocally attributed to enhanced biosynthetic activity per cell. Furthermore, the elevated extracellular nucleic acid and protein levels in Ca^{2+}-treated cultures do not constitute direct evidence of altered membrane permeability. The transcriptomic data, while providing a descriptive overview of the transcriptional landscape, may be partially confounded by physiological differences between the Ca^{2+}-treated and control cultures, including differences in growth rate and biomass accumulation. Collectively, these findings suggest that Ca^{2+} promotes fungal growth and is associated with increased bostrycin accumulation, but definitive conclusions regarding the specific activation of bostrycin biosynthesis require further biomass-normalized and functionally validated studies. This work provides a foundational dataset for understanding Ca^{2+}-associated physiological and transcriptional responses in *N. sphaerica* HCH285 and may inform future metabolic engineering efforts.

Acknowledgements

Not applicable.

Authors' contributions

BYY: Formal analysis, Data curation, Writing – original draft, Writing – review & editing. SSZ: Investigation, Formal analysis. WYZ: Validation. YZL: Conceptualization, Methodology. XXD: Supervision. YH: Supervision. ZQW: Supervision,Funding acquisition,Conceptualization, Writing – review & editing. FX: Conceptualization, Methodology, Writing – review & editing.

Funding

This research was funded by the Emerging Interdisciplinary Research Funding of WHPU (No. WHPU-EIRF-2606), Natural Science Foundation of Hubei Province (Grant No. 2023AFB968) and the Hubei-Key-Laboratory of Industrial, Microbiology (Grant No. 2024KF07).

Data availability

The datasets generated and analysed during the current study are available in the NCBI Sequence Read Archive (SRA) under BioProject accession PRJNA1543448 (https://dataview.ncbi.nlm.nih.gov/object/PRJNA1543448). All other data generated or analysed during this study are included in this published article and its supplementary information files.

Declarations

Ethics approval and consent to participate

Not applicable.

Consent for publication

Not applicable.

Competing interests

The authors declare no competing interests.

References

[1] M. S. Butler and J. J. La Clair, “The Role of Natural Product Chemistry in Drug Discovery: Two Decades of Progress and Perspectives,” *J Nat Prod*, vol. 89, no. 1, pp. 3–28, Jan. 2026, doi: 10.1021/acs.jnatprod.5c01368.

[2] S. Hadid, E. Zhang, W. H. Frishman, and E. Brutsaert, “Insulin’s Legacy: A Century of Breakthroughs and Innovation,” *Cardiol Rev*, vol. 34, no. 3, pp. 204–211, Jun. 2026, doi: 10.1097/CRD.0000000000000680.

[3] M. K. Bilonda and L. Mammino, “Intramolecular Hydrogen Bonds in Conformers of Quinine and Quinidine: An HF, MP2 and DFT Study,” *Molecules*, vol. 22, no. 2, Feb. 2017, doi: 10.3390/molecules22020245.

[4] E. L. Dulaney, “Observations on Streptomyces Griseus. III. Carbon Sources for Growth and Streptomycin Production,” *Mycologia*, vol. 41, no. 1, 1949, doi: 10.2307/3755267.

[5] J. R. Willdigg *et al.*, “The Bacillus subtilis cell envelope stress-inducible ytpAB operon modulates membrane properties and contributes to bacitracin resistance,” *J Bacteriol*, vol. 206, no. 3, p. e0001524, Mar. 2024, doi: 10.1128/jb.00015-24.

[6] R. Gaynes, “The Discovery of Penicillin—New Insights After More Than 75 Years of Clinical Use,” *Emerg Infect Dis*, vol. 23, no. 5, pp. 849–853, May 2017, doi: 10.3201/eid2305.161556.

[7] A. P. Nath, A. Balasubramanian, and K. Ramalingam, “Cephalosporins : An imperative antibiotic over the generations,” *International Journal of Research in Pharmaceutical Sciences*, vol. 11, no. 1, pp. 623–630, Jan. 2020, doi: 10.26452/ijrps.v11i1.1866.

[8] F. B. Mortzfeld, C. Hashem, K. Vranková, M. Winkler, and F. Rudroff, “Pyrazines: Synthesis and Industrial Application of these Valuable Flavor and Fragrance Compounds,” *Biotechnology Journal*, vol. 15, no. 11, p. 2000064, 2020, doi: 10.1002/biot.202000064.

[9] D. Tang *et al.*, “Engineered Microbial Consortium for De Novo Production of Sclareolide,” *J Agric Food Chem*, vol. 72, no. 36, pp. 19977–19984, Sep. 2024, doi: 10.1021/acs.jafc.4c05506.

[10] L. Yang, H. Liu, Y. Jin, J. Liu, L. Deng, and F. Wang, “Recent Advances in Multiple Strategies for the Synthesis of Terpenes by Engineered Yeast,” *Fermentation*, vol. 8, no. 11, Nov. 2022, doi: 10.3390/fermentation8110615.

[11] F. Cao *et al.*, “A target and efficient synthetic strategy for structural and bioactivity optimization of a fungal natural product,” *Eur J Med Chem*, vol. 229, p. 114067, Feb. 2022, doi: 10.1016/j.ejmech.2021.114067.

[12] H. Chen *et al.*, “Studies on the Synthesis of Derivatives of Marine-Derived Bostrycin and Their Structure-Activity Relationship against Tumor Cells,” *Marine Drugs*, vol. 10, no. 4, pp. 932–952, Apr. 2012, doi: 10.3390/md10040932.

[13] W.-S. Chen *et al.*, “Bostrycin inhibits proliferation of human lung carcinoma A549 cells via downregulation of the PI3K/Akt pathway,” *J Exp Clin Cancer Res*, vol. 30, no. 1, p. 17, Feb. 2011, doi: 10.1186/1756-9966-30-17.

[14] C. Xu *et al.*, “The anthracenedione compound bostrycin induces mitochondria-mediated apoptosis in the yeast Saccharomyces cerevisiae,” *FEMS Yeast Res*, vol. 10, no. 3, pp. 297–308, May 2010, doi: 10.1111/j.1567-1364.2010.00615.x.

[15] J. Li *et al.*, “Optimal fermentation time for Nigrospora-fermented tea rich in bostrycin,” *J*

Sci Food Agric, vol. 101, no. 6, pp. 2483–2490, Apr. 2021, doi: 10.1002/jsfa.10874.

[16] J. Macheleidt *et al.*, "Regulation and Role of Fungal Secondary Metabolites," *Annu Rev Genet*, vol. 50, pp. 371–392, Nov. 2016, doi: 10.1146/annurev-genet-120215-035203.

[17] M. Chen *et al.*, "Effect of metal ions on lipopeptide secretion from Bacillus subtilis strain FJAT-4: Negative regulation by Ca^{2+}," *J. Appl. Microbiol.*, vol. 132, no. 3, pp. 2167–2176, Mar. 2022, doi: 10.1111/jam.15347.

[18] L. Karaffa, E. Fekete, and C. P. Kubicek, "The Role of Metal Ions in Fungal Organic Acid Accumulation," *Microorganisms*, vol. 9, no. 6, Jun. 2021, doi: 10.3390/microorganisms9061267.

[19] A. S. Abbas and C. Edwards, "Effects of Metals on Streptomyces coelicolor Growth and Actinorhodin Production," *Appl Environ Microbiol*, vol. 56, no. 3, pp. 675–680, Mar. 1990, doi: 10.1128/aem.56.3.675-680.1990.

[20] L. F. Dobson and D. G. O'Shea, "Antagonistic effect of divalent cations Ca^{2+} and Mg^{2+} on the morphological development of Streptomyces hygroscopicus var. geldanus," *Appl Microbiol Biotechnol*, vol. 81, no. 1, pp. 119–126, Nov. 2008, doi: 10.1007/s00253-008-1627-7.

[21] T. Zhou *et al.*, "Enhanced cercosporin production by co-culturing Cercospora sp. JNU001 with leaf-spot-disease-related endophytic bacteria," *Microb Cell Fact*, vol. 20, no. 1, p. 100, May 2021, doi: 10.1186/s12934-021-01587-2.

[22] H. Li and J.-J. Zhong, "Role of calcineurin-responsive transcription factor CRZ1 in ganoderic acid biosynthesis by *Ganoderma lucidum*," *Process Biochemistry*, vol. 95, pp. 166–173, Aug. 2020, doi: 10.1016/j.procbio.2020.05.027.

[23] W.-J. Yang, C.-S. Yang, C.-J. Huang, K.-S. Chen, and S.-F. Lin, "Bostrycin, a novel coupling agent for protein immobilization and prevention of biomaterial-centered infection produced by Nigrospora sp. No. 407," *Enzyme Microb Technol*, vol. 50, no. 6–7, pp. 287–292, May 2012, doi: 10.1016/j.enzmictec.2012.02.002.

[24] N. Suwannarach *et al.*, "Optimization and characterization of red pigment production from an endophytic fungus, Nigrospora aurantiaca CMU-ZY2045, and its potential source of natural dye for use in textile dyeing," *Appl Microbiol Biotechnol*, vol. 103, no. 17, pp. 6973–6987, Sep. 2019, doi: 10.1007/s00253-019-09926-5.

[25] S. Lu *et al.*, "A Network of Sporogenesis-Responsive Genes Regulates the Growth, Asexual Sporogenesis, Pathogenesis and Fusaric Acid Production of Fusarium oxysporum f. sp. cubense," *Journal of Fungi*, vol. 10, no. 1, Dec. 2023, doi: 10.3390/jof10010001.

[26] T. B. Pedersen *et al.*, "Heterologous Expression of the Core Genes in the Complex Fusarubin Gene Cluster of Fusarium Solani," *Int J Mol Sci*, vol. 21, no. 20, p. 7601, Oct. 2020, doi: 10.3390/ijms21207601.

[27] Q. Li, Y. Zhao, X. Zhu, and Y. Xie, "Antifungal efficacy of paeonol on *Aspergillus flavus* and its mode of action on cell walls and cell membranes," *LWT*, vol. 149, p. 111985, Sep. 2021, doi: 10.1016/j.lwt.2021.111985.

[28] Y. Yue *et al.*, "Antifungal mechanisms of volatile organic compounds produced by *Pseudomonas fluorescens* ZX as biological fumigants against *Botrytis cinerea*," *Microbiological Research*, vol. 267, p. 127253, Feb. 2023, doi: 10.1016/j.micres.2022.127253.

[29] M. Ashburner *et al.*, "Gene ontology: tool for the unification of biology. The Gene Ontology

Consortium," *Nat Genet*, vol. 25, no. 1, pp. 25–29, May 2000, doi: 10.1038/75556.
[30] M. Kanehisa, M. Furumichi, Y. Sato, M. Kawashima, and M. Ishiguro-Watanabe, "KEGG for taxonomy-based analysis of pathways and genomes," *Nucleic Acids Res*, vol. 51, no. D1, pp. D587–D592, Jan. 2023, doi: 10.1093/nar/gkac963.
[31] K. J. Livak and T. D. Schmittgen, "Analysis of relative gene expression data using real-time quantitative PCR and the 2(-Delta Delta C(T)) Method," *Methods*, vol. 25, no. 4, pp. 402–408, Dec. 2001, doi: 10.1006/meth.2001.1262.
[32] Y. Zhao *et al.*, "Physiological, biochemical, and global transcriptomic and metabolomic analyses of the effect of the antifungal compound isobavachalcone on *Botrytis cinerea* on cherry tomatoes," *LWT*, vol. 204, p. 116467, Jul. 2024, doi: 10.1016/j.lwt.2024.116467.
[33] X. Tong, Q.-T. Wang, X.-Y. Shen, C.-L. Hou, and P. F. Cannon, "Phylogenetic Position of Shiraia-Like Endophytes on Bamboos and the Diverse Biosynthesis of Hypocrellin and Hypocrellin Derivatives," *Journal of Fungi*, vol. 7, no. 7, Jul. 2021, doi: 10.3390/jof7070563.
[34] X. Yi *et al.*, "Taurine-mediated gene transcription and cell membrane permeability reinforced co-production of bioethanol and Monascus azaphilone pigments for a newly isolated Monascus purpureus," *Biotechnol Biofuels Bioprod*, vol. 17, no. 1, p. 59, May 2024, doi: 10.1186/s13068-024-02511-7.
[35] G. Xie *et al.*, "SZ-685C, a marine anthraquinone, is a potent inducer of apoptosis with anticancer activity by suppression of the Akt/FOXO pathway," *Br J Pharmacol*, vol. 159, no. 3, pp. 689–697, Feb. 2010, doi: 10.1111/j.1476-5381.2009.00577.x.

Supplementary Files

This is a list of supplementary files associated with this preprint. Click to download.

- SupplementaryInformation.docx